EOMES is responsible for WNT memory and can substitute for WNT in mesendoderm specification

Anna Yoney[1,2,4,5], Lu Bai[3,4], Ali H. Brivanlou[2,*], Eric D. Siggia[1,*]

[1]Center for Studies in Physics and Biology, The Rockefeller University, New York, NY 10065, USA

[2]Laboratory of Stem Cell biology and Molecular Embryology, The Rockefeller University, New York, NY 10065, USA

[3]Department of Biochemistry and Molecular Biology, Department of Physics, Center for Eukaryotic Gene Regulation, The Pennsylvania State University, University Park, PA, 16802, USA

[4]Contributed equally

[5]Current address: Department of Genetics and Development, Columbia University, New York, NY 10032

*Correspondence: brvnlou@rockefeller.edu (A.H.B.), siggiae@rockefeller.edu (E.D.S)

Abstract

Embryogenesis is guided by a limited set of signaling pathways that are reused at different times and places throughout development. How a context dependent signaling response is generated has been a central question of developmental biology, which can now be addressed with *in vitro* model systems. Our previous work in human embryonic stem cells (hESCs) established that pre-exposure of cells to WNT/β-catenin signaling is sufficient to switch the output of ACTIVIN/SMAD2 signaling from pluripotency maintenance to mesendoderm (ME) differentiation. A body of previous literature has established the role of both pathways in ME differentiation. However, our work demonstrated that the two signals do not need to be present simultaneously and that hESCs have a means to record WNT signals. Here we demonstrate that hESCs have accessible chromatin at SMAD2 binding sites near pluripotency and ME-associated target genes and that WNT priming does not alter SMAD2 binding. Rather our results indicate that stable transcriptional output at ME genes results from WNT-dependent production of an additional SMAD2 co-factor, EOMES. We show that expression of EOMES can replace WNT signaling in ME differentiation, providing a mechanistic basis for WNT-priming and memory in early development.

Introduction

Understanding self-renewal vs differentiation of human embryonic stem cells (hESCs) is a critical step in elucidating human development. The ACTIVIN/NODAL signaling pathway, mediated by transcription factors SMAD2/3, plays dual roles in this process. On one hand, nuclear SMAD2/3 promotes the expression of pluripotency factors *OCT4* and *NANOG* and is essential for hESC pluripotency maintenance (James et al. 2005; Vallier, Alexander, and Pedersen 2005; Vallier et al. 2009); on the other hand, in combination with WNT/β-catenin signaling, SMAD2/3 can induce hESC differentiation into primitive streak and mesendoderm (ME) derivatives (Sumi et al. 2008; Singh et al. 2012; Loh et al. 2014; Funa et al. 2015; Estarás, Benner, and Jones 2015), including human organizer tissue (Martyn et al. 2018). Our previous paper revealed that the exit of pluripotency in the latter case requires a signaling cascade of WNT acting upstream of ACTIVIN: hESCs "primed" with WNT for 24 hours with subsequent exposure to ACTIVIN can differentiate into ME cells, while each signaling pathway alone is unable to induce this differentiation (Yoney et al. 2018). We also showed that ACTIVIN induces transient influx of SMAD2 into the nucleus and that the SMAD2 nuclear entry/exit dynamics are not affected by the WNT stimulation (Yoney et al. 2018). It is, thus, unclear how WNT priming alters the hESC response to SMAD2 signaling to give rise to the ME fate.

There are a few molecular mechanisms, which could explain our observation of signal priming of hESCs. WNT signaling can generate a co-factor that physically interacts with SMAD2 to stabilize its binding on DNA and/or direct it to different genomic loci (Funa et al. 2015); it can introduce a coactivator that does not affect SMAD2 binding but enhances SMAD2 activity at the transcriptional level (Estarás, Benner, and Jones 2015); it may inhibit a SMAD2 repressor, allowing it to activate ME specific genes; finally, WNT may induce epigenetic changes of chromatin that facilitate SMAD2 binding and/or transcriptional activation. Previous studies on ME differentiation have typically applied WNT and ACTIVIN/NODAL simultaneously (Sumi et al. 2008;

Loh et al. 2014; Estarás, Benner, and Jones 2015; Martyn et al. 2018). Our finding that these two signaling pathway can be temporally separated provides new ways to decouple and manipulate the differentiation process. Here, using our stepwise protocol, we investigated the mechanism of coordination between WNT and ACTIVIN during ME differentiation.

Results

WNT functions temporally up-stream of ACTIVIN to specify mesendoderm. We have previously shown that WNT and ACTIVIN signaling are both required to induce ME from pluripotent hESCs but that the signals can be presented in temporal succession: 24 h WNT3A (WNT) followed by 24 h ACTIVIN A (ACTIVIN or ACT) (Yoney et al. 2018). With this protocol (WNT → ACT), we observed significant reduction of *SOX2* expression and strong induction of ME marker genes, *BRACHYURY*, *EOMES*, and *GSC* (Figure 1A–B). WNT signals appeared to "prime" cells rather than cause a stable fate change since the pluripotency markers OCT, NANOG and SOX2 but no ME markers were detected at the protein level after 24 h of WNT (Yoney et al. 2018). Although *EOMES* and *BRA* transcripts were induced by 24 h of WNT, these levels were significantly lower than those induced by WNT followed by ACTIVIN (Figure 1B). Furthermore, when cells were primed with WNT and then cultured in base medium (E7) without WNT or ACTIVIN for an additional 24 h, ME transcript levels did not continue to increase (Figure 1B) nor was protein expression detected (Yoney et al. 2018). These features characterize what we call the WNT-primed state of hESCs.

Differentiation protocols often use a small molecule, CHIR99021 (CHIR), in place of recombinant WNT protein to activate the canonical pathway (Kunisada et al. 2012; Naujok et al. 2014). CHIR inhibits GSK3, thus preventing it from triggering the degradation of the WNT signaling effector β-CATENIN. Our standard WNT priming assay worked similarly with 24 h CHIR presentation followed by 24 h ACTIVIN, indicating that priming happens at the level of β-CATENIN stabilization

or downstream of it (Figure S1A). In our protocol we cultured single cells in base medium overnight prior to WNT priming in order remove SMAD2-activating signals that are present in hESC maintenance cultures. Therefore, in order to address the possibility that cells require both signals in close succession but not in a particular temporal order, we treated cells with ACTIVIN for 24 hours, washed, and then immediately stimulated with WNT for an additional 24 h. We did not observe ME induction using the reverse order or with either signal alone (Figure S1B). Taken together, these results demonstrate that WNT priming through β-CATENIN acts up-stream of ACTIVIN signaling to specify the ME fate.

In other studies, 1-2 days of WNT stimulation or GSK3 inhibition was sufficient to induce BRA protein expression (Funa et al. 2015; Martyn, Brivanlou, and Siggia 2019; Diaz-Cuadros et al. 2020). We attribute the absence of BRA protein in our protocol to the use of low-density cell culture, which we hypothesize prevents cells from responding to endogenously produced WNT and ACTIVIN/NODAL ligands and consequently reduces the level of BRA transcripts produced after 24 h of exogenous WNT. To test this hypothesis, we treated cells grown in confluent micropatterned cell culture with the same conditions that we used to define the WNT primed state in low-density cultures (Figure 1A). We detected expression of BRA, EOMES, and GSC at the protein level after 24 h of WNT, which in the case of EOMES and GSC increases further after an additional 24 h in ACTIVIN or E7 (Figure S2A–B). Cells positive for ME markers were enriched at the colony borders as expected from our previous studies on WNT and TGFβ signaling in this system (Warmflash et al. 2014; Etoc et al. 2016; Yoney et al. 2018; Martyn, Brivanlou, and Siggia 2019). ME markers were strongly reduced when micropatterned colonies were treated with WNT in the presence of inhibitors of ACTIVIN/NODAL signaling, SB431542 (SB), and endogenous WNT secretion, IWP-2, and cells instead remained pluripotent as indicated by the maintenance of SOX2 (Figure S2C–D). These results imply that the activity of endogenous signals account for

differences in timing of ME differentiation between high- and low-density hESC cultures and demonstrate that low density cultures allow for more precise manipulation of signals.

Global transcriptome analysis reveals that WNT priming regulates the expression of a small subset of SMAD2/3-target genes. The above experiments confirm our original observation that hESCs have a differential transcriptional response to ACTIVIN with or without WNT priming. We then performed bulk RNA-sequencing on the complete set of conditions (Figure 1A) to examine the transcriptional response at the genome-wide scale. The 1212 genes that showed a significant change in expression in at least one of the conditions relative to 24 h in E7 (n=2 biological replicates, adjusted P-value < 0.01) were clustered by their response across all conditions (Figure 1C). Among all differentially expressed genes, we observed a significant change in 189 of them after 24h of WNT presentation (n = 2 biological replicates, adjusted P-value < 0.01). Highly induced genes in the 24 h WNT condition, including *EOMES*, *BRA*, and *NODAL*, partially reverse to their basal level after a subsequent 24 h in E7 without WNT or ACTIVIN, which further supports our hypothesis based on rt-PCR and immunofluorescence data that WNT signals prime cells rather than cause them to undergo a stable fate change (Figure 1B and Figure S1A–B). 24 h ACTIVIN induced mild transcriptional changes. Importantly, for the pluripotency maker genes, including *NANOG*, *OCT4*, *SOX2*, and *KLF4*, their expression either remained constant or was upregulated in both the WNT and ACT conditions, confirming the lack of differentiation with either signal alone. When ACTIVIN was applied subsequent to WNT, we observed more extensive changes in the global transcriptional response, including 661 upregulated genes and 383 downregulated genes, which implies more extensive differentiation of the cells to ME. Overall, the RNA-seq results are consistent with the rt-PCR measurements in Figure 1B.

In our previous study we showed that the application of ACTIVIN to the hESCs induces transient translocation of SMAD2 and SMAD4 into the nucleus, which elicits a transcriptional change in ~3500 genes (Yoney et al. 2018). Many of the differentially expressed genes are activated rapidly following SMAD2/4 translocation, suggesting that they are direct targets of these transcription factors. Among the genes that are activated within 4 h after ACTIVIN presentation, most of them quickly return to their pre-stimulation level with the drop in SMAD2/4 nuclear concentration (pulsing genes), while a small fraction shows sustained expression (stable genes). We further divided the pulsing and stable genes based on how they responded to WNT priming (Figure S3). We found 93 pulsing and 20 stable genes that show significantly higher mRNA levels in WNT → ACT condition compared to WNT → E7 (primed) or E7 → ACT (pluripotent) conditions, indicating that these genes respond to the cooperative signaling of WNT and ACTIVIN. This group of 113 genes includes *EOMES*, *BRACHYURY*, *GSC, MIXL1*, *GATA6 and NODAL*, which is consistent with previous reports that β-CATENIN and SMAD2/3 co-regulate expression of genes that are expressed within the primitive streak and ME derivatives (Estarás, Benner, and Jones 2015; Funa et al. 2015). The remaining 2285 pulsing and 35 stable genes that we identified in our previous RNA-seq dataset did not change their long-term behavior, i.e., at 24 h after ACTIVIN, following WNT priming (Figure S3).

In summary our genome-wide transcriptional analyses support the idea that WNT reversibly primes pluripotent hESCs for differentiation and that together, WNT and ACTIVIN drive cells towards a committed ME fate. We were able to unbiasedly identify groups of ACTIVIN/SMAD2 target genes, whose transcriptional response is affected by WNT priming. In our subsequent analyses, we will compare groups of ACTIVIN/SMAD2 target genes, those that are WNT priming dependent vs independent, with respect to additional features, including the presence of other transcription factor (TF) binding sites and changes in chromatin accessibility, in order to further dissect the mechanism of WNT priming.

Cells retain a memory of WNT priming. Motivated by the observations of "WNT memory" in other species ranging from flies to frog (Blythe et al. 2010; Alexandre, Baena-Lopez, and Vincent 2013), we further explored our original hypothesis that hESCs also possess the ability to record WNT signals. In order to demonstrate extended WNT memory, we stimulated cells with WNT for 24 h, followed by one day in medium lacking WNT or ACTIVIN (E7) before switching to ACTIVIN for 24 h. We included SB to prevent the cells from responding to endogenous ACTIVIN/NODAL signals as the cell density increases. As we have previously shown, SB treatment during WNT priming had little effect on the subsequent induction of ME markers by ACTIVIN (Figure 1D) (Yoney et al. 2018). WNT priming in the presence of SB followed by an additional day in E7+SB and then ACTIVIN also resulted in the induction of the ME markers EOMES and BRA and loss of pluripotency as indicated by the down regulation of SOX2 (Figure 1D). We observed a quantitative reduction in the "memory" with respect to the level of EOMES induction and SOX2 repression. Nevertheless, these results show that WNT priming of hESCs is retained for at least 24 h after removal of the signal, which is on the order of one cell cycle, and points to a mechanism of WNT memory that is slowly lost in individual cells.

SMAD2 binds to the same loci with or without WNT priming. In our previous study, we found that the SMAD2 concentration and nuclear entry-exit dynamics are not affected by WNT priming (Yoney et al. 2018). Consistent with this result, the RNA-seq data above show that WNT only primes a small fraction of ACTIVIN target genes, indicating that WNT does not globally modify SMAD2 activity. How then does WNT priming modify the cellular response to ACTIVIN?

SMADs have weak DNA specificity and often rely on co-factors to be directed to target regions on the genome in a cell-type specific manner (Massagué 2012). For example, SMAD2 binding in hESCs depends on OCT4 and NANOG, but during endoderm differentiation it is recruited to

different genomic loci through interactions with EOMES and GATA6 (Teo et al. 2011; Brown et al. 2011; Li et al. 2019). We therefore first tested the hypothesis that WNT priming causes SMAD2 to bind to different genomic locations. We analyzed the SMAD2/3 ChIP-seq data in Kim et al., 2011 (ChIP in H9 ESCs in conditioned media, which is close to our E7/ACT condition) and in Tsankov et al., 2015 (ChIP in ME cells generated with WNT + ACT treatment for 12 h, which is close to our WNT/ACT condition). Surprisingly, despite the difference in transcriptional profile, SMAD2/3 ChIP-seq peaks are largely overlapping between these two conditions (Figure 2A), which is consistent with previous SMAD2/3 ChIP analyses in pluripotent hESCs vs hESC derived endoderm cells (Brown et al. 2011). For example, the mRNA levels for *GSC*, *MIXL1*, *CER1*, and *GATA4* are orders of magnitude higher in WNT/ACT than E7/ACT condition, but their SMAD2 ChIP-seq patterns are very similar in these two conditions (Figure S4).

The published SMAD2/3 ChIP data were performed in cell lines and conditions that are different from ours. In addition, they assayed binding at time points that are late relative to the peak SMAD2 nuclear accumulation following ACTIVIN stimulation (Yoney et al. 2018). To verify that the same conclusions can be drawn in our experimental conditions and to examine the possibility that WNT priming influences SMAD2 binding at earlier time points, which could result in differences in transcript levels at later time points, we selected a few SMAD2 binding regions near genes that respond to WNT priming (*GSC*, *CER1*, and *NODAL*) and carried out ChIP-qPCR measurements (Figure 2B). For all genes tested, we observed an increase in SMAD2 binding at 2 h relative to 24 h following ACTIVIN presentation. However, the level of binding is comparable with or without WNT priming. This analysis indicates that higher SMAD2 nuclear concentration promotes SMAD2 binding at target genes. However, SMAD2 binding *per se* is not correlated with transcriptional output and corresponding changes in cell fate.

SMAD2 leads to comparable level of chromatin opening with or without WNT priming. Given that SMAD2 can bind to the same genes with or without WNT priming but activates them to a different extent, it is possible that SMAD2 may have different activation potentials for different genes with or without WNT priming. Because TF activation is often accompanied by local chromatin opening, we carried out ATAC-seq to probe the changes in chromatin accessibility around TF binding sites. The ATAC-seq experiments were performed in the same conditions described above for RNA-seq (Figure 1A) with the E7 condition again used to calculate relative changes. The ATAC-seq profiles in all conditions are very similar showing that there is no global rearrangement of open chromatin regions in the transition from pluripotency to ME differentiation (Figure S5A–B). Furthermore, a vast majority of genes contain ATAC-seq peaks near their TSS and within transcript regions, regardless of their transcriptional status (Figure S5C).

Despite the global similarities, there are quantitative changes in the ATAC signals over specific TF binding sites. For β-CATENIN, the ATAC-seq data clearly show that its binding sites are highly accessible before in E7 media, prior to WNT stimulation (Figure 3A). After 24 h WNT treatment, β-CATENIN associates with these pre-opened chromatin regions and further enhances the ATAC signals (Figure 3B). The level of enhancement correlates with β-CATENIN binding strength determined from ChIP-seq peak area (Estarás, Benner, and Jones 2015). Interestingly, such enhancement is reduced in the WNT → E7 sample, indicating that β-CATENIN dissociates from chromatin after WNT wash-out. In addition, the ATAC peaks drop to the same level in the WNT → ACT as in the WNT → E7 condition, suggesting that the presence of nuclear SMAD2 does not retain β-CATENIN on chromatin (Figure 3B).

We performed the same analysis using SMAD2 binding sites. Note that we used both sets of SMAD2 ChIP data (Kim et al. 2011; Tsankov et al. 2015), although the two sets are highly similar (Figure 2A). This subset of ATAC signals is essentially identical in E7 and WNT conditions,

indicating that WNT signaling does not alter the chromatin environment near SMAD2 binding sites. In contrast, with both E7 → ACT and WNT → ACT treatment, ATAC-seq signals are enhanced over SMAD2 binding sites, and the level of enhancement correlates with SMAD2 binding strength (Figure 3C–D). Therefore, such enhancement likely results from SMAD2 binding and subsequent opening of the local chromatin. Importantly, such enhancement is similar in E7 → ACT and WNT → ACT, indicating that the activity of chromatin opening by SMAD2 is not dependent on WNT priming.

Nuclear β-CATENIN is insufficient to drive ME differentiation with SMAD2. We have shown that WNT priming affects neither SMAD2 binding nor its ability to open chromatin. It has been proposed that the main TF that responds to WNT signaling, β-CATENIN, functions as a co-activator of SMAD2, either through direct physical interaction (Funa et al. 2015) or cooperatively by recruiting RNA pol II (Estarás, Benner, and Jones 2015). β-CATENIN indeed tends to bind WNT-primed genes together with SMAD2 (Figure S6A–B). It is thus possible that during ACTIVIN treatment after WNT priming, the remaining β-CATENIN nuclear fraction cooperates with newly translocated SMAD2 to drive the expression of key ME genes (Figure 4A).

Two pieces of evidence argue against this scenario. First, β-CATENIN rapidly accumulates in the nucleus after WNT presentation, reaching the peak concentration at ~6h (Massey et al. 2019). If the overlap between nuclear β-CATENIN and SMAD2/4 is the key for WNT priming, a shorter period of WNT treatment should be sufficient for ME differentiation. However, 6h of WNT priming followed by 24h of ACTIVIN is not able to activate ME genes (Figure 4B). The fact that WNT priming requires longer time strongly indicates that a product resulting from β-CATENIN activation, instead of β-CATENIN itself, is essential to turn on the ME differentiation program with ACTIVIN/SMAD2.

Second, we tested if the overlap between β-CATENIN and SMAD2 is necessary for ME differentiation. We repeated our WNT/ACT protocol but now added the drug endo-IWR1 at varying times from 0 to 12 h after the addition of Activin (Figure 5A). This drug triggers the degradation of β-CATENIN and therefore should control its overlap with SMAD2. Some genes are less activated by ACTIVIN when endo-IWR1 was added immediately after WNT treatment (0h), but the effect of the drug is much attenuated when added at later time points (4h, 8h, and 12h) (Figure 5B–C). Importantly, marker genes for definitive endoderm (DE), including *SOX17*, *GATA4*, and *FOXA2*, are also induced, indicating that ESCs can differentiate into more mature endoderm after the elimination of β-CATENIN. Combined with Figure 4, we conclude that the presence of β-CATENIN in the nucleus is not sufficient to start the ME program, and after 24h WNT priming, long-term overlap between β-CATENIN and SMAD2 is also not necessary for ME differentiation.

EOMES is a potential effector for WNT priming. From the results above, we hypothesized that WNT priming generates another TF that functions as an essential SMAD2 co-regulator. Given our data in Figures 4 and 5, we suspect that this TF should be activated by 24 h of WNT treatment, and its expression should be further enhanced by the brief overlap of β-CATENIN and SMAD2 in the WNT → ACT condition. If that is the case, we expect this TF to bind in proximity to WNT-primed genes in a WNT → ACT specific manner. Accordingly, we probed the binding signature of this TF by searching for enhanced ATAC peaks that require the combined action of WNT and ACTIVIN. In contrast to the general consistency of the ATAC peaks under various conditions, there was a statistically significant subset of 3983 peaks that are enhanced in WNT → ACT in comparison to both E7 → ACT and WNT → E7 (Figure 6A). The probabilities for such peaks to fall within 20k bp of WNT-primed genes in both the pulsing and stable ACTIVIN categories are significantly higher than the ones that are not primed by WNT, indicating that these ATAC-seq peaks correlate with transcriptional activation and therefore, are likely to represent enhancers (Figure 6B).

We analyzed motifs that are enriched in these WNT → ACT enhanced ATAC peaks, both genome-wide and the subset that is proximal to WNT-primed genes. In both cases, we found the EOMES motif to be the most significantly enriched motif (Figure 6C). Consistent with our expectation, EOMES is activated by WNT alone and becomes highly expressed in WNT → ACT condition (Figure 1B). EOMES tends to bind closely to SMAD2 in the vicinity of WNT-primed genes (Figure S6C–D), and it is essential for ESCs to differentiate into ME cells, including definitive endoderm (Teo et al. 2011; Li et al. 2019). In contrast, the TF with the second most enriched motif, BRACHYURY (Figure 6C), is not essential for ME differentiation (Tosic et al. 2019; Li et al. 2019). Of the remaining significantly enriched motifs that we found, the only other motif corresponding to a specific TF family belongs to the GATA family. GATA4/6 are key endoderm TFs, but their expression is not upregulated with 24 h WNT (supporting data for Figure 1C). Therefore, we conclude that EOMES is the most likely effector of WNT priming.

Exogenous EOMES expression bypasses WNT priming to induce ME differentiation. If EOMES is the key factor mediating WNT priming, the prediction is that we can bypass WNT priming and achieve ME differentiation by artificially expressing EOMES. To test this hypothesis we generated RUES2 hESC lines with doxycycline(dox)-inducible *EOMES* using the piggyBac transposon system (*TT-EOMES*) (Lacoste, Berenshteyn, and Brivanlou 2009) (Figure S7A). Titration experiment shows that *TT-EOMES* is induced in these cells in a dox concentration- and time-dependent manner (Figure S7B). In particular, 6 h treatment with 0.1 μg/mL dox induces EOMES protein expression to a level comparable to the endogenous levels in our ME protocol (Figure S7B–C). According to previous studies, *EOMES* expression in the absence of ACTIVIN drives cells towards cardiac mesoderm fate by activating *MESP1*, and addition of ACTIVIN inhibits cardiac differentiation (van den Ameele et al. 2012). We observed the same trend of *MESP1* expression in our dox-treated TT-EOMES lines in the presence or absence of ACTIVIN (Figure

S7D). To avoid this unintended differentiation pathway, dox was applied in the presence of ACTIVIN in the protocol below.

We next tested the ability of EOMES to differentiate cells towards ME in the absence of WNT by inducing *TT-EOMES* for 6 h with 0.05, 0.1, and 0.2 μg/mL dox in the presence of ACTIVIN, washing out dox, and measuring gene expression at different time points after dox removal (Figure 7A). This protocol generates a pulse of *TT-EOMES* expression, as its level decreases rapidly following the removal of dox (Figure 7B). Such transient *TT-EOMES* expression induced by 0.1 and 0.2 μg/mL, but not 0.05 μg/mL dox, was sufficient to drive the full complement of ME and DE genes, including the endogenous *EOMES*, at levels that match those obtained with WNT → ACT treatment of the wild-type, parental cell line (Figure 7C). Note that ME genes like *EOMES* and *GSC* are activated earlier than DE genes like *SOX17*, indicating that the cells driven by *TT-EOMES* go through a normal differentiation process. EOMES can also induce the expression of *WNT3* (Figure S7E) (Pfeiffer et al. 2018). To eliminate the possibility that *TT-EOMES* drives hESC differentiation through the production of endogenous WNT, we repeated our experiments in the presence of endo-IWR1. When applied to the unmodified hESCs in the WNT →ACT protocol, endo-IWR1 completely blocks the activation of ME genes (Yoney et al. 2018). In contrast, endo-IWR1 has little effect on the ME gene expression driven by *TT-EOMES* (Figure 7D). These results strongly suggest that EOMES is the effector of WNT priming, and exogenously expressed EOMES can drive ME differentiation in the absence of WNT signaling.

There are three isoforms of human *EOMES*, and the experiments above were performed using the long isoform, isoform 1 (Figure S8A). Isoform 2 differs from isoform 1 by only a few amino acids, and the shorter isoform 3 skips an exon in the N-terminal. All three isoforms contain the T-box DNA binding domain and the transcriptional activation domain, and we found reads supporting both the short and long isoforms in our RNA-seq data from the WNT → ACT condition.

We generated a second hESC line with dox-inducible *EOMES* isoform 3. Although the expression level of *TT-EOMES*(3) in this line is much lower even in the presence of saturating dox, we were able to induce differentiation using transient dox induction. In this case, the cells expressed higher levels of *BRA* and lower levels of other ME and DE makers (Figure S8B–C). These differences may be due to lower protein concentration independent of the specific isoform and/or inefficiency of this isoform at driving ME differentiation. Overall, our results provide a molecular mechanism of WNT priming and indicate that *EOMES* expression is sufficient to switch the output of ACTIVIN signaling from pluripotency maintenance to ME differentiation.

Discussion

In this work we provide a mechanism for our previous observation that WNT signaling primes hESCs to differentiate in response to ACTIVIN signaling (Yoney et al. 2018). We propose that the main function of WNT priming is to generate a sufficient level of EOMES that drives ME differentiation together with SMAD2. EOMES binds to its own promoter, and it was proposed that it can activate itself to maintain a high expression level during ME induction (Teo et al. 2011; Kartikasari et al. 2013). For hESCs to initiate this positive feedback loop, we propose that EOMES expression needs to reach a critical level, either through sustained WNT signaling in wild-type hESCs (Figure 5B, 24 h WNT but not 6 h is sufficient) or sufficient induction of *TT-EOMES* in our modified cell line (Figure 7B–C, requires >0.05 μg/mL dox for 6 h). While there is prior literature showing EOMES is a cofactor for SMAD2 in ME differentiation, we specifically found EOMES and SMAD2 co-binding enriched in genes sensitive to WNT priming (Figure S6), which establishes a critical link between WNT and ACT signaling in ME differentiation. Our proposed mechanism for WNT priming is summarized in Figure 8.

Chromatin modifications have long been implicated in cellular memory as the term epigenetics implies. In *Xenopus* a delay between Wnt signaling and transcriptional onset was linked to an

epigenetic mechanism in which β-CATENIN recruits a histone methyltransferase to target genes and is required for their activation at the mid-blastula transition (Blythe et al. 2010). The competence of the *Xenopus* blastula to respond to Wnt signals was also shown to have a chromatin component (Esmaeili et al. 2020). Closer to our study, Tosic et al. showed that EOMES and BRA are required for ME gene expression in mouse and that their binding is associated with open chromatin. Wnt memory specifically was invoked in surprising experiments in the fly wing where it was shown that tethered Wnt had a very minor phenotype (Alexandre, Baena-Lopez, and Vincent 2013). Instead of spreading from the localized source at the DV boundary in the late wing, cells remember their earlier exposure when the wing disk was much smaller and Wnt signaling more widespread. Yet no mechanism was given for the memory. We did not find evidence for drastic changes in chromatin opening with WNT priming. However, it is still possible that histone modifications play a role in WNT priming and memory during differentiation of hESCs, with EOMES potentially recruiting the epigenetic modifiers (Kartikasari et al. 2013).

In our prior work we began by dissecting the interaction of Wnt and Activin/Nodal in mesendoderm. Here we report that induction of EOMES at near physiological levels can replace the requirement for Wnt in ME induction and it does so without the involvement of β-CATENIN signaling. This extends prior work that places EOMES at the top of a hierarchy of TFs that along with SMAD2/3 regulate ME differentiation in mouse and humans (Teo et al. 2011; Kartikasari et al. 2013; Li et al. 2019). Interestingly, mutual activation of EOMES and WNT3 drives cardiac differentiation, an alternative pathway that is repressed by ACTIVIN/SMAD2 signaling (van den Ameele et al. 2012; Pfeiffer et al. 2018). Thus, signaling pathways and the key TFs which they activate create reciprocal context-dependent states that drive cellular differentiation during development.

Materials and methods

ATAC-sequencing: Chromatin accessibility profiling was carried out using the Omni-ATAC-sequencing protocol as an attempt to reduce mitochondrial DNA in our samples (Corces et al. 2017). We obtained single cells using Gentle Cell Dissociation Reagent (STEMCELL Technologies), rather than Accutase or other enzyme-based reagents, which we found disrupted downstream processing steps. Cells (100,000 per condition) were resuspended in 50 µL lysis buffer (0.1% NP-40, 0.1% Tween-20, 0.01% Digitonin) prepared in resuspension buffer (10 mM Tris-HCl pH 7.4, 10 mM NaCl, and 3 mM $MgCl_2$ in water) for 3 minutes on ice. We optimized the lysis time so that the outer membrane was disrupted as indicated by Trypan blue staining of the nuclei but that the nuclei remained intact. The lysis buffer was removed by washing with 0.1% Tween-20 in resuspension buffer, and the transposition was subsequently carried out in 50 µL reaction volume containing 25 µL 2X TD buffer and 2.5 µL Tn5 transposase (available as individual products upon request from Illuminia). The transposition reaction was incubated at 37 °C for 30 minutes in a thermomixer set to 1,000 r.p.m. The transposed DNA was isolated using the Qiagen MinElute kit and was eluted in 30 µL of water in the final step. Library preparation was carried out using 10 µL of transposed DNA per sample as described previously with 10 - 11 cycles of amplification (Buenrostro et al. 2015). Our DNA tended to be under digested, so we performed doubled-sided bead purification using AMPure XP beads (Beckman). Libraries were sequenced as paired-end 75 bp reads, multiplexing all samples per experiment (7) on one lane of the Illumina High-Seq 500 platform at The Rockefeller University Genomics Resource Center. Two biological replicates for each condition were collected, processed, and sequenced from independent experiments.

ChIP: For ChIP experiment in Figure 2B, we used a SMAD2/3 antibody (R&D systems, AF3797) in 2X10^6 hESCs that were treated with ACTIVIN for 2 h or 24 h with or without WNT priming. We used the Pierce™ magnetic ChIP kit and followed the procedure provided by the kit. Known Smad2 binding sites near *GSC*, *NODAL*, and *CER1* genes were selected for subsequent qPCR

analysis based on previously published SMAD2/3 ChIP-seq data (Kim et al. 2011; Tsankov et al. 2015). A region near *CER1* gene that has low SMAD2/3 ChIP-seq signal was chosen as the negative control.

Bioinformatics analysis: RNAseq data were aligned by Rsubread, and the read count associated with genes were analyzed by featureCounts. The differential fold changes and effective p-values were obtained using DESeq2. The data in Figure 1C and Table 1 include those genes that show a significant change (adjusted p-value < 0.01) in at least one of the four conditions relative to E7: (1) E7→ACT, (2) 24 h WNT, (3) WNT→E7, or (4) WNT→ACT. The k-mean clustering was done using MATLAB *kmeans* function.

The ChIP-seq and ATACseq data were aligned with bowtie2 for the hg19 reference genome and visualized using deepTools bamCoverage function. The peaks were identified using MACS2 narrow peak calling. The area underneath the peak (like in Figure 2A, 3B, and 3D) were calculated using MultiCovBed function. The heatmaps in Figure 3A and C were generated using deepTools computeMatrix and plotHeatmap. The differential peaks in Figure 6A were identified using DESeq2 based on the areas underneath each peak. In Figure 6B, we collected the TSSs and TESs of genes in different categories (pulsing/stable) and examined if there are any WNT → ACT enhanced ATAC-seq peaks fall between 20kb upstream TSSs and 20kb downstream the TESs. The enriched motifs in the WNT → ACT enhanced ATAC-seq peaks were identified by AME with the HOCOMOCOv10 database against other ATAC-seq peaks that are not sensitive to the WNT → ACT condition.

Data and software availability: Published datasets used in this study include β-CATENIN ChIP data (GSM1579346), SMAD2/3 ChIP data from pluripotent hESCs (GSM727557), SMAD2/3 ChIP data from human mesendoderm cells differentiated from hESCs (GSM1505750), and EOMES

ChIP data (GSM1505630 and GSM1505631). The RNA-seq and ATAC-seq data generated from this study have been deposited in NCBI's Gene Expression Omnibus.

Acknowledgements

This work is supported by R35 GM139654 to LB and R01 GM101653 to EDS and AHB.

References

Alexandre, Cyrille, Alberto Baena-Lopez, and Jean Paul Vincent. 2013. “Patterning and Growth Control by Membrane-Tethered Wingless.” *Nature* 505 (7482). Nature Publishing Group: 180–85. doi:10.1038/nature12879.

Blythe, Shelby A, Sang-Wook Cha, Emmanuel Tadjuidje, Janet Heasman, and Peter S Klein. 2010. “B-Catenin Primes Organizer Gene Expression by Recruiting a Histone H3 Arginine 8 Methyltransferase, Prmt2.” *Developmental Cell* 19 (2): 220–31. doi:10.1016/j.devcel.2010.07.007.

Brown, Stephanie, Adrian Teo, Siim Pauklin, Nicholas Hannan, Candy H-H Cho, Bing Lim, Leah Vardy, et al. 2011. “Activin/Nodal Signaling Controls Divergent Transcriptional Networks in Human Embryonic Stem Cells and in Endoderm Progenitors.” *Stem Cells* 29 (8). John Wiley & Sons, Ltd: 1176–85. doi:10.1002/stem.666.

Buenrostro, Jason D, Beijing Wu, Howard Y Chang, and William J Greenleaf. 2015. “ATAC-Seq: a Method for Assaying Chromatin Accessibility Genome-Wide.” *Current Protocols in Molecular Biology* 109 (1). John Wiley & Sons, Ltd: 21.29.1–21.29.9. doi:10.1002/0471142727.mb2129s109.

Clevers, Hans, Kyle M Loh, and Roel Nusse. 2014. “An Integral Program for Tissue Renewal and Regeneration: Wnt Signaling and Stem Cell Control.” *Science* 346 (6205). American Association for the Advancement of Science: 1248012. doi:10.1126/science.1248012.

Corces, M Ryan, Alexandro E Trevino, Emily G Hamilton, Peyton G Greenside, Nicholas A Sinnott-Armstrong, Sam Vesuna, Ansuman T Satpathy, et al. 2017. “An Improved ATAC-Seq Protocol Reduces Background and Enables Interrogation of Frozen Tissues.” *Nature Methods* 14 (10). Nature Publishing Group: 959–62. doi:10.1038/nmeth.4396.

Diaz-Cuadros, Margarete, Daniel E Wagner, Christoph Budjan, Alexis Hubaud, Oscar A Tarazona, Sophia Donelly, Arthur Michaut, et al. 2020. “In Vitro Characterization of the Human Segmentation Clock.” *Nature* 580 (7801). Nature Publishing Group: 113–18. doi:10.1038/s41586-019-1885-9.

Esmaeili, Melody, Shelby A Blythe, John W Tobias, Kai Zhang, Jing Yang, and Peter S Klein. 2020. “Chromatin Accessibility and Histone Acetylation in the Regulation of Competence in Early Development.” *bioRxiv* 12 (January). Cold Spring Harbor Laboratory: 797183. doi:10.1101/797183.

Estarás, Conchi, Chris Benner, and Katherine A Jones. 2015. “SMADs and YAP Compete to Control Elongation of B-Catenin:LEF-1-Recruited RNAPII During hESC Differentiation.” *Molecular Cell* 58 (5): 780–93. doi:10.1016/j.molcel.2015.04.001.

Etoc, Fred, Jakob Metzger, Albert Ruzo, Christoph Kirst, Anna Yoney, M Zeeshan Ozair, Ali H Brivanlou, and Eric D Siggia. 2016. “A Balance Between Secreted Inhibitors and Edge Sensing Controls Gastruloid Self-Organization.” *Developmental Cell* 39 (3). Elsevier: 302–15. doi:10.1016/j.devcel.2016.09.016.

Funa, Nina S, Karen A Schachter, Mads Lerdrup, Jenny Ekberg, Katja Hess, Nikolaj Dietrich, Christian Honoré, Klaus Hansen, and Henrik Semb. 2015. “B-Catenin Regulates Primitive Streak Induction Through Collaborative Interactions with SMAD2/SMAD3 and OCT4.” *Cell Stem Cell* 16 (6): 639–52. doi:10.1016/j.stem.2015.03.008.

James, Daylon, Ariel J Levine, Daniel Besser, and Ali Hemmati-Brivanlou. 2005. “TGFbeta/Activin/Nodal Signaling Is Necessary for the Maintenance of Pluripotency in Human Embryonic Stem Cells..” *Development* 132 (6): 1273–82. doi:10.1242/dev.01706.

Kartikasari, Apriliana E R, Josie X Zhou, Murtaza S Kanji, David N Chan, Arjun Sinha, Anne Grapin-Botton, Mark A Magnuson, William E Lowry, and Anil Bhushan. 2013. “The Histone Demethylase Jmjd3 Sequentially Associates with the Transcription Factors Tbx3 and Eomes to Drive Endoderm Differentiation..” *The EMBO Journal* 32 (10). John Wiley & Sons, Ltd: 1393–1408. doi:10.1038/emboj.2013.78.

Kim, Si Wan, Se-Jin Yoon, Edward Chuong, Chuba Oyolu, Andrea E Wills, Rakhi Gupta, and Julie Baker. 2011. “Chromatin and Transcriptional Signatures for Nodal Signaling During Endoderm Formation in hESCs..” *Developmental Biology* 357 (2): 492–504. doi:10.1016/j.ydbio.2011.06.009.

Kunisada, Yuya, Noriko Tsubooka-Yamazoe, Masanobu Shoji, and Masaki Hosoya. 2012. “Small Molecules Induce Efficient Differentiation Into Insulin-Producing Cells From Human Induced Pluripotent Stem Cells..” *Stem Cell Research* 8 (2): 274–84. doi:10.1016/j.scr.2011.10.002.

Lacoste, Arnaud, Frada Berenshteyn, and Ali H Brivanlou. 2009. “An Efficient and Reversible Transposable System for Gene Delivery and Lineage-Specific Differentiation in Human

Embryonic Stem Cells." *Cell Stem Cell* 5 (3). Cell Press: 332–42. doi:10.1016/j.stem.2009.07.011.

Li, Qing V, Gary Dixon, Nipun Verma, Bess P Rosen, Miriam Gordillo, Renhe Luo, Chunlong Xu, et al. 2019. "Genome-Scale Screens Identify JNK–JUN Signaling as a Barrier for Pluripotency Exit and Endoderm Differentiation." *Nature Genetics* 51 (6). Nature Publishing Group: 999–1010. doi:10.1038/s41588-019-0408-9.

Loh, Kyle M, Lay Teng Ang, Jingyao Zhang, Vibhor Kumar, Jasmin Ang, Jun Qiang Auyeong, Kian Leong Lee, et al. 2014. "Efficient Endoderm Induction From Human Pluripotent Stem Cells by Logically Directing Signals Controlling Lineage Bifurcations.." *Cell Stem Cell* 14 (2): 237–52. doi:10.1016/j.stem.2013.12.007.

Martyn, I, T Y Kanno, A Ruzo, E D Siggia, and A H Brivanlou. 2018. "Self-Organization of a Human Organizer by Combined Wnt and Nodal Signalling." *Nature* 558 (7708). Nature Publishing Group: 132–35. doi:10.1038/s41586-018-0150-y.

Martyn, Iain, Ali H Brivanlou, and Eric D Siggia. 2019. "A Wave of WNT Signaling Balanced by Secreted Inhibitors Controls Primitive Streak Formation in Micropattern Colonies of Human Embryonic Stem Cells." *Development* 146 (6). Oxford University Press for The Company of Biologists Limited: dev172791. doi:10.1242/dev.172791.

Massagué, Joan. 2012. "TGFβ Signalling in Context." *Nature Reviews Molecular Cell Biology* 13 (10). Nature Publishing Group: 616–30. doi:10.1038/nrm3434.

Massey, Joseph, Yida Liu, Omar Alvarenga, Teresa Saez, Matthew Schmerer, and Aryeh Warmflash. 2019. "Synergy with TGFβ Ligands Switches WNT Pathway Dynamics From Transient to Sustained During Human Pluripotent Cell Differentiation." *Proceedings of the*

National Academy of Sciences 116 (11). National Academy of Sciences: 4989–98. doi:10.1073/pnas.1815363116.

Naujok, Ortwin, Jana Lentes, Ulf Diekmann, Claudia Davenport, and Sigurd Lenzen. 2014. "Cytotoxicity and Activation of the Wnt/Beta-Catenin Pathway in Mouse Embryonic Stem Cells Treated with Four GSK3 Inhibitors." *BMC Research Notes* 7 (1). BioMed Central: 1–8. doi:10.1186/1756-0500-7-273.

Pfeiffer, Martin J, Roberto Quaranta, Ilaria Piccini, Jakob Fell, Jyoti Rao, Albrecht Röpke, Guiscard Seebohm, and Boris Greber. 2018. "Cardiogenic Programming of Human Pluripotent Stem Cells by Dose-Controlled Activation of EOMES." *Nature Communications* 9 (1). Nature Publishing Group: 1–8. doi:10.1038/s41467-017-02812-6.

Singh, Amar M, David Reynolds, Timothy Cliff, Satoshi Ohtsuka, Alexa L Mattheyses, Yuhua Sun, Laura Menendez, Michael Kulik, and Stephen Dalton. 2012. "Signaling Network Crosstalk in Human Pluripotent Cells: a Smad2/3-Regulated Switch That Controls the Balance Between Self-Renewal and Differentiation.." *Cell Stem Cell* 10 (3): 312–26. doi:10.1016/j.stem.2012.01.014.

Sumi, Tomoyuki, Norihiro Tsuneyoshi, Norio Nakatsuji, and Hirofumi Suemori. 2008. "Defining Early Lineage Specification of Human Embryonic Stem Cells by the Orchestrated Balance of Canonical Wnt/Beta-Catenin, Activin/Nodal and BMP Signaling." *Development* 135 (17): 2969–79. doi:10.1242/dev.021121.

Teo, Adrian Kee Keong, Sebastian J Arnold, Matthew W B Trotter, Stephanie Brown, Lay Teng Ang, Zhenzhi Chng, Elizabeth J Robertson, N Ray Dunn, and Ludovic Vallier. 2011. "Pluripotency Factors Regulate Definitive Endoderm Specification Through Eomesodermin.." *Genes & Development* 25 (3): 238–50. doi:10.1101/gad.607311.

Tosic, Jelena, Gwang-Jin Kim, Mihael Pavlovic, Chiara M Schröder, Sophie-Luise Mersiowsky, Margareta Barg, Alexis Hofherr, et al. 2019. “Eomes and Brachyury Control Pluripotency Exit and Germ-Layer Segregation by Changing the Chromatin State.” *Nature Cell Biology* 21 (12). Nature Publishing Group: 1518–31. doi:10.1038/s41556-019-0423-1.

Tsankov, Alexander M, Hongcang Gu, Veronika Akopian, Michael J Ziller, Julie Donaghey, Ido Amit, Andreas Gnirke, and Alexander Meissner. 2015. “Transcription Factor Binding Dynamics During Human ES Cell Differentiation.” *Nature* 518 (7539). Nature Publishing Group: 344–49. doi:10.1038/nature14233.

Vallier, Ludovic, Morgan Alexander, and Roger A Pedersen. 2005. “Activin/Nodal and FGF Pathways Cooperate to Maintain Pluripotency of Human Embryonic Stem Cells.” *Journal of Cell Science* 118 (19). The Company of Biologists Ltd: 4495–4509. doi:10.1242/jcs.02553.

Vallier, Ludovic, Sasha Mendjan, Stephanie Brown, Zhenzhi Chng, Adrian Teo, Lucy E Smithers, Matthew W B Trotter, et al. 2009. “Activin/Nodal Signalling Maintains Pluripotency by Controlling Nanog Expression.” *Development* 136 (8): 1339–49. doi:10.1242/dev.033951.

van den Ameele, Jelle, Luca Tiberi, Antoine Bondue, Catherine Paulissen, Adèle Herpoel, Michelina Iacovino, Michael Kyba, Cédric Blanpain, and Pierre Vanderhaeghen. 2012. “Eomesodermin Induces Mesp1 Expression and Cardiac Differentiation from Embryonic Stem Cells in the Absence of Activin.” *EMBO Reports* 13 (4). John Wiley & Sons, Ltd: 355–62. doi:10.1038/embor.2012.23.

Warmflash, Aryeh, Benoit Sorre, Fred Etoc, Eric D Siggia, and Ali H Brivanlou. 2014. “A Method to Recapitulate Early Embryonic Spatial Patterning in Human Embryonic Stem Cells.” *Nature Methods* 11 (8). Nature Research: 847–54. doi:10.1038/nmeth.3016.

Yoney, Anna, Fred Etoc, Albert Ruzo, Thomas Carroll, Jakob J Metzger, Iain Martyn, Shu Li, Christoph Kirst, Eric D Siggia, and Ali H Brivanlou. 2018. “WNT Signaling Memory Is Required for ACTIVIN to Function as a Morphogen in Human Gastruloids.” *eLife* 7 (October). eLife Sciences Publications Limited. doi:10.7554/eLife.38279.

Figure legends

Figure 1. WNT priming and memory in hESCs. A) Experimental conditions used to induce a WNT-primed or mesendoderm state (ME). Cells are treated with 100 ng/mL WNT3A (WNT) and 10 ng/mL ACTIVIN A (ACT), either alone or sequentially, in E7 medium. **B)** Expression of ME genes (*EOMES*, *BRA*, *GSC*) and pluripotent genes (*NANOG*, *OCT4*, *SOX2*) measured by rt-PCR in cells treated with the experimental conditions defined in (A). Data points represent the mean fold change relative to E7 for independent biological replicates. Bars and error bars represent the mean ± S.D., respectively, across n = 2 or 3 biological replicates. Differences between means that were determined to be significant are shown (*P<0.05, **P< 0.01, ***P<0.001, ANOVA). **C)** *k*-means clustering of RNA-seq data measured in 4 conditions (columns) revealed 4 clusters that could be annotated as follows: genes for which the expression increases in all conditions in which ACTIVIN is present (cluster 1, n = 415), all conditions in which WNT is present (cluster 2, n = 224), or further activated by WNT+ACT (higher induction in WNT/ACT than WNT or ACT alone, cluster 3, n = 137). The fourth cluster represents genes that are repressed by the WNT/ACT condition (cluster 4, n = 435). The intensities represent log2 fold change of expression relative to the E7 condition. Only genes showing a significant change (adjusted p-value < 0.01) in at least one condition relative to E7 were included in the heatmap and clustering procedure. **D)** Memory of the WNT-primed state was tested by incubating cells for an additional day in E7 in the presence of SB431542 (SB, 10 μM) prior to presenting ACTIVIN (10 ng/mL). SB was used to eliminate ACTIVIN signaling during the first 48 h. After 24 h of ACTIVIN stimulation, cells were fixed and analyzed by immunofluorescence (IF) for EOMES, BRA, and SOX2 expression. Histograms showing the nuclear IF signal quantified in single cells (n > 5,000 cells per condition).

Figure 2. SMAD2 binds the same genomic loci with or without WNT priming. A) SMAD2 ChIP peak intensity in ESCs vs. ME. The ChIP peaks were called either with data from pluripotent hESCs (Kim et al. 2011) or from hESCs derived ME cells (Tsankov et al. 2015). Independent of the cell type in which the peaks were called the levels of SMAD2 binding, measured by peak area, are similar in pluripotent hESCs and ME cells. R, Pearson correlation. **B)** SMAD2 ChIP signals over previously known SMAD2 binding sites near *GSC*, *CER1*, and *NODAL* genes, as well as a negative control region that does not show SMAD2 binding in the genome-wide datasets. The ChIP measurements were performed at 2 or 24 hours after ACTIVIN (10 ng/mL) application with or without WNT priming. The ChIP signal was normalized by the total input. Data represents the mean ± S.D. for n = 2 technical replicates.

Figure 3. SMAD2 shows similar chromatin opening activity with or without WNT priming. **A)** ATAC-seq signals centered at β-CATENIN binding sites measured in five conditions indicated at the top. Rows represent genomic regions sorted by the β-CATENIN ChIP peak intensities (Estarás, Benner, and Jones 2015). **B)** Fold change of the ATAC-seq signals over the β-CATENIN binding sites in four conditions relative to E7. The five bars in each condition represent 5 quantiles of β-CATENIN binding strength. **C**) Same as in (A) except that ATAC-seq signals are centered at SMAD2/3 binding sites based on ChIP data from pluripotent hESCs (Kim et al. 2011). **D)** Same as in (B) except that the five bars represent 5 quantiles of SMAD2/3 binding strength (based on ChIP data in either pluripotent hESCs or ME cells).

Figure 4. Presence of nuclear β-CATENIN is not sufficient for ME differentiation. A) Schematic depicting the hypothesis to be tested that increased ME gene expression requires overlap of β-CATENIN and SMAD2/3. Cartoon showing the nuclear concentration of β-CATENIN and SMAD2 during the WNT/ACT treatment. **B)** Short WNT exposure is not sufficient to prime the cells for ME differentiation. Cells were treated for different amounts of time with WNT (100 ng/mL) prior to adding ACTIVIN (10 ng/mL). IWP2, which prevents cells from secreting WNT ligands, is used in this protocol to ensure that WNT signaling is restricted to the first 6 h. After 24 h of ACTIVIN stimulation, cells were fixed and analyzed by immunofluorescence for EOMES, BRA, and GSC expression. Histograms showing the nuclear IF signal quantified in single cells (n > 5,000 cells per condition).

Figure 5. Long-term overlap between β-CATENIN and SMAD2 is not necessary for ME differentiation. A) Protocol for testing the effect of different amounts of β-CATENIN/SMAD2 overlap on ME differentiation. We applied endo-IWR1 at different time points during the ACTIVIN phase, which continues to the end. The nuclear concentration of β-CATENIN is reduced by endo-IWR1, thus reducing its overlap with SMAD2. **B**–**C)** rt-PCR analysis of (B) ME and DE genes or (C) pluripotent genes after 24h or 48h of ACTIVIN treatment (10 ng/mL) with endo-IWR1 added at different time points. Expression levels after standard E7/ACT and WNT/ACT treatment (negative and positive control, respectively) are also shown. Expression in each sample was normalized to GAPDH and then to the pluripotency levels (E7/ACT, 24h). Data represents the mean ± S.D. for n = 3 technical replicates.

Figure 6. EOMES motif is enriched in WNT/ACT-enhanced ATAC peaks. A) Heatmap of the ATAC-seq signals that are enhanced in WNT/ACT condition in comparison to WNT or ACT alone. **B)** Probability of finding these WNT/ACT-enhanced peaks near pulsing or stable genes (start of the gene - 20kb to end of the gene + 20kb) that are either sensitive or insensitive to WNT priming. ***: p-value < 10^{-4}, *: p-value <10^{-2}. **C)** EOMES motif is the most enriched motif, followed by BRACHYURY (BRA) found in the WNT/ACT-enhanced peaks near genes that are WNT primed.

Figure 7. Exogenous EOMES expression bypasses WNT priming to induce ME differentiation. A) Protocol to assay ME differentiation in response to a pulse of TT-EOMES expression induced by doxycycline (dox). **B**–**C)** Time course analysis of (B) *TT-EOMES* and (C) endogenous ME and DE gene expression following transient *TT-EOMES* induction (6 h with variable dox concentration). Cells were collected at 0, 12, 24, and 48h during the ACTIVIN phase for rt-PCR measurements. Data points represent the mean fold change relative to pluripotency levels in the parental line (E7/ACT). The expression levels in wild-type parental cell line treated with WNT followed by ACT for 24 h or 48 h are shown for comparison. Bars represent the mean across n = 2 biological replicates. § expression in the parental line was not measured for these genes/time points. **D)** Similar to (B) except that endo-IWR1 (1 μM) was added to block WNT signaling. The bar plots show the mRNA levels of ME genes at different time points during the ACT phase with or without endo-IWR1.

Figure 8. EOMES is the main effector of WNT priming. (A) WNT signaling through β-CATENIN induces low levels of EOMES expression, which are further boosted by additional factors including SMAD2/3 and EOMES itself. When EOMES levels are sufficiently high, its expression can be maintained in the absence of WNT/β-CATENIN. **(B)** Likewise, sufficiently high levels of EOMES together with SMAD2/3 can drive additional genes required for complete ME differentiation.

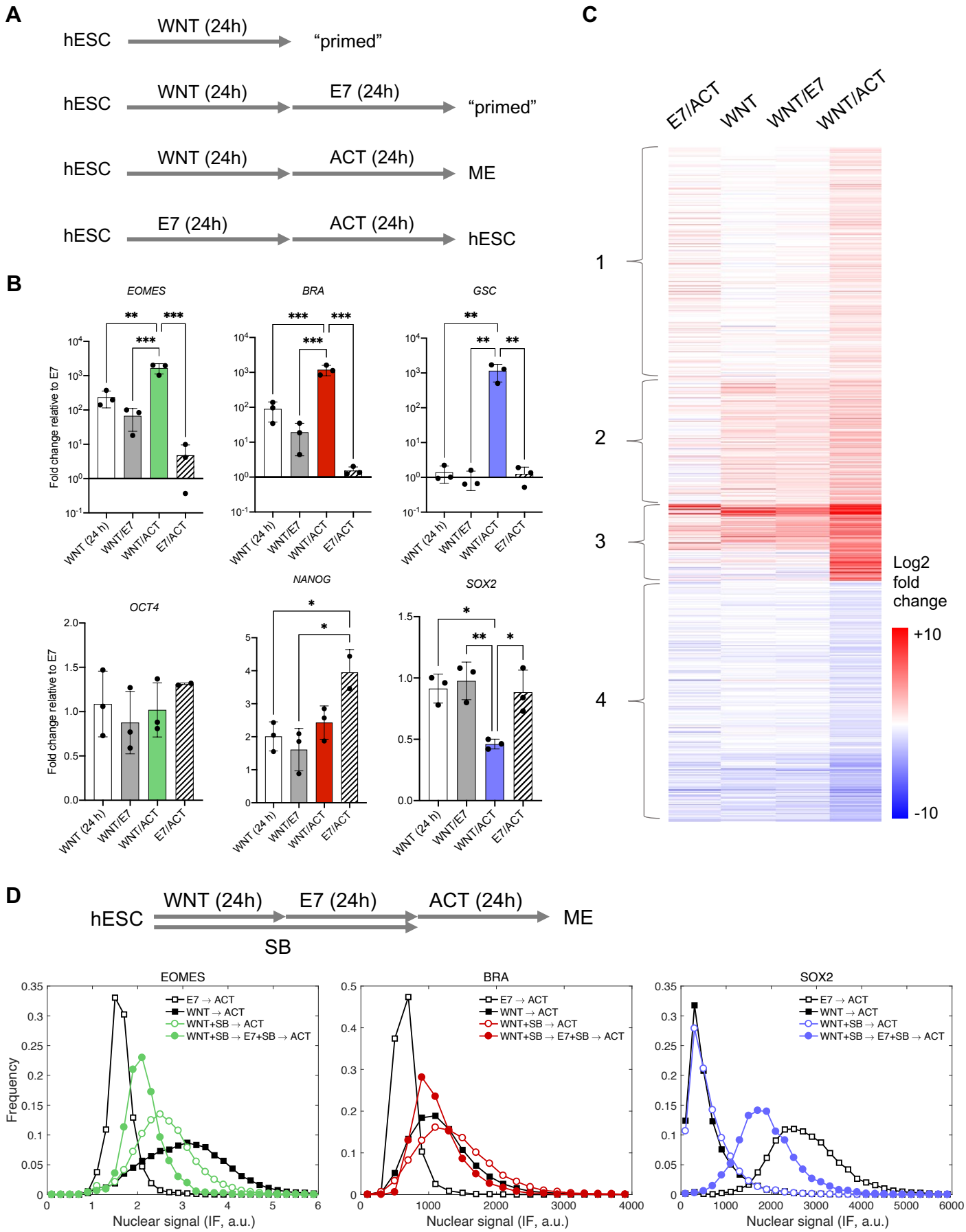
A
hESC
WNT (24h)
"primed"
hESC
WNT (24h)
E7 (24h)
"primed"
hESC
WNT (24h)
ACT (24h)
ME
hESC
E7 (24h)
ACT (24h)
hESC
B
EOMES
BRA
GSC
OCT4
NANOG
SOX2
Fold change relative to E7
WNT (24 h)
WNT/E7
WNT/ACT
E7/ACT
C
E7/ACT
WNT
WNT/E7
WNT/ACT
1
2
3
4
Log2 fold change
+10
-10
D
hESC
WNT (24h)
E7 (24h)
ACT (24h)
ME
SB
EOMES
BRA
SOX2
E7 → ACT
WNT → ACT
WNT+SB → ACT
WNT+SB → E7+SB → ACT
Frequency
Nuclear signal (IF, a.u.)

Figure 1

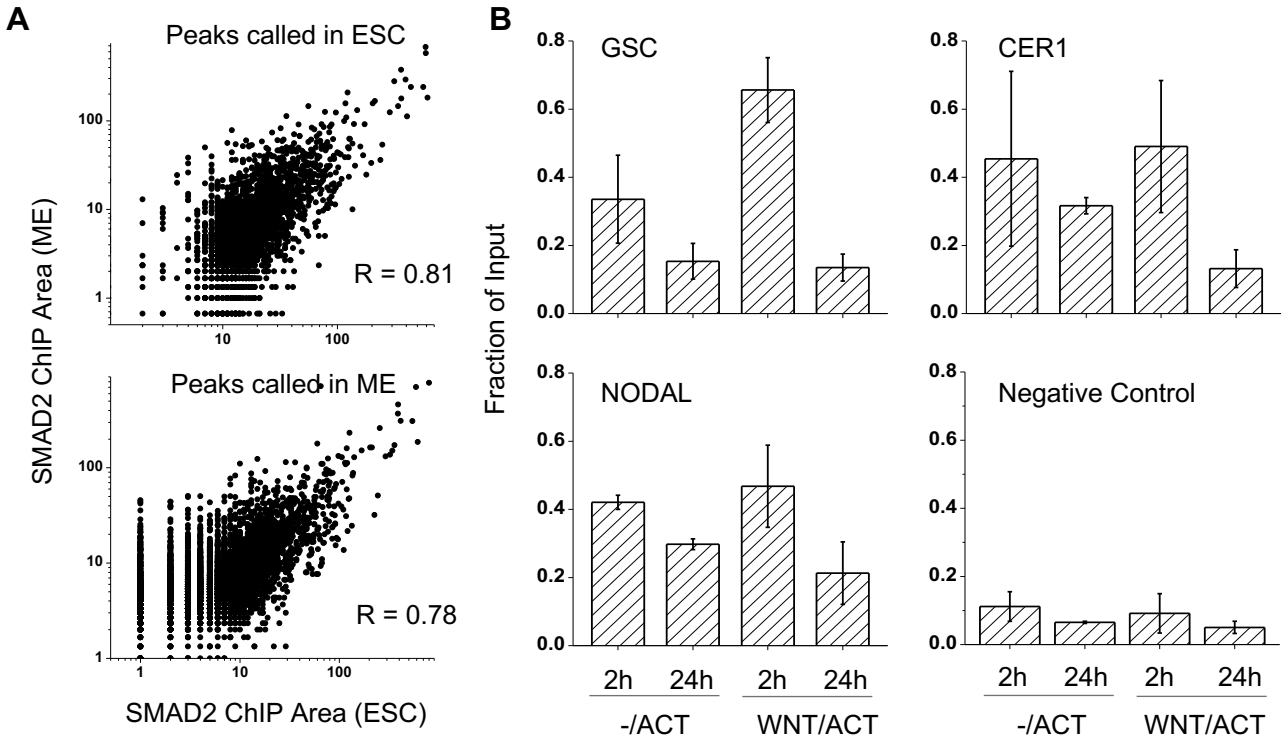
A
Peaks called in ESC
R = 0.81
Peaks called in ME
R = 0.78
SMAD2 ChIP Area (ME)
SMAD2 ChIP Area (ESC)
B
GSC
CER1
NODAL
Negative Control
Fraction of Input
2h
24h
-/ACT
WNT/ACT

Figure 2

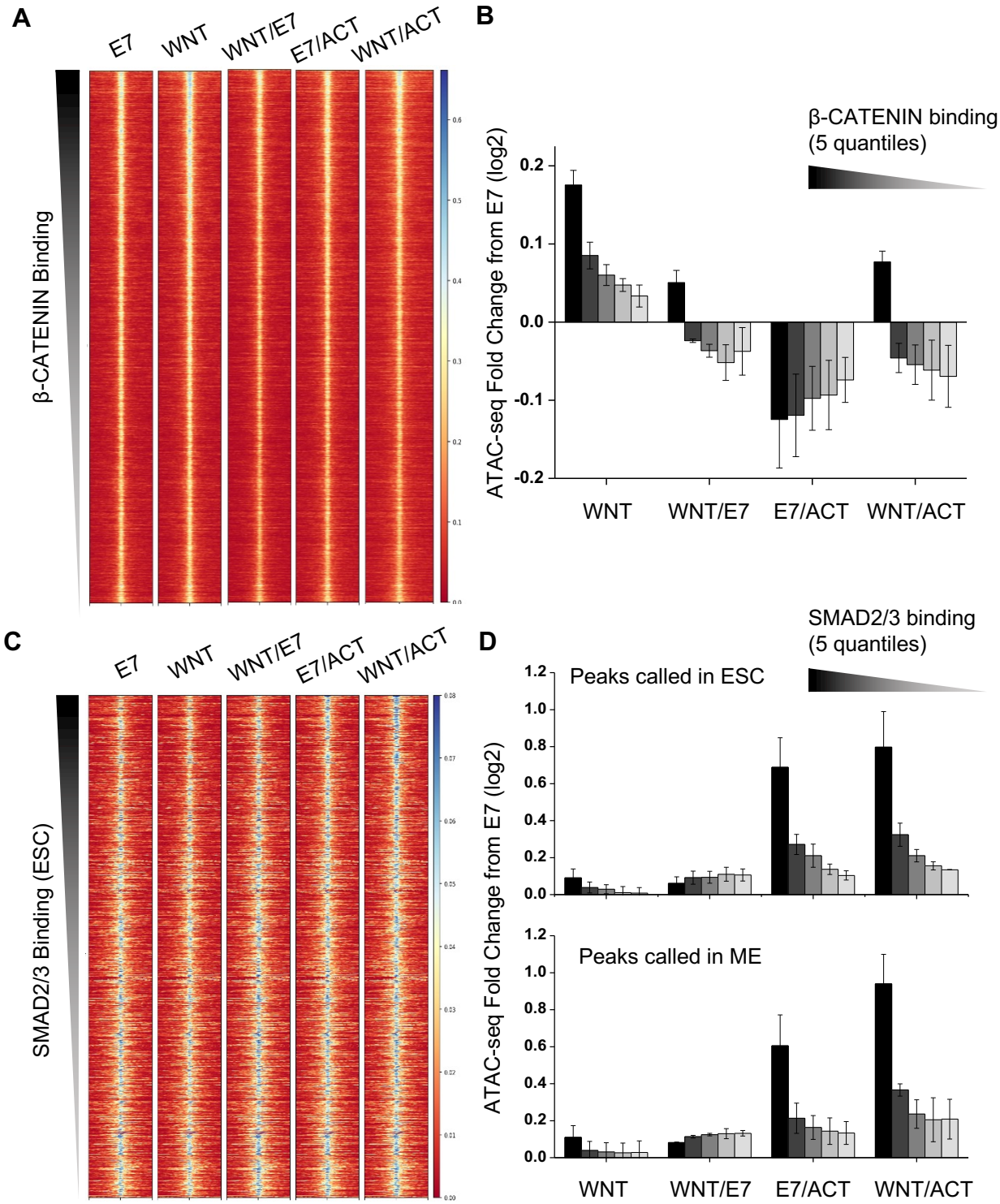
A
E7
WNT
WNT/E7
E7/ACT
WNT/ACT
β-CATENIN Binding
B
β-CATENIN binding
(5 quantiles)
ATAC-seq Fold Change from E7 (log2)
0.2
0.1
0.0
-0.1
-0.2
WNT
WNT/E7
E7/ACT
WNT/ACT
C
E7
WNT
WNT/E7
E7/ACT
WNT/ACT
SMAD2/3 Binding (ESC)
D
SMAD2/3 binding
(5 quantiles)
Peaks called in ESC
Peaks called in ME
ATAC-seq Fold Change from E7 (log2)
1.2
1.0
0.8
0.6
0.4
0.2
0.0
WNT
WNT/E7
E7/ACT
WNT/ACT

Figure 3

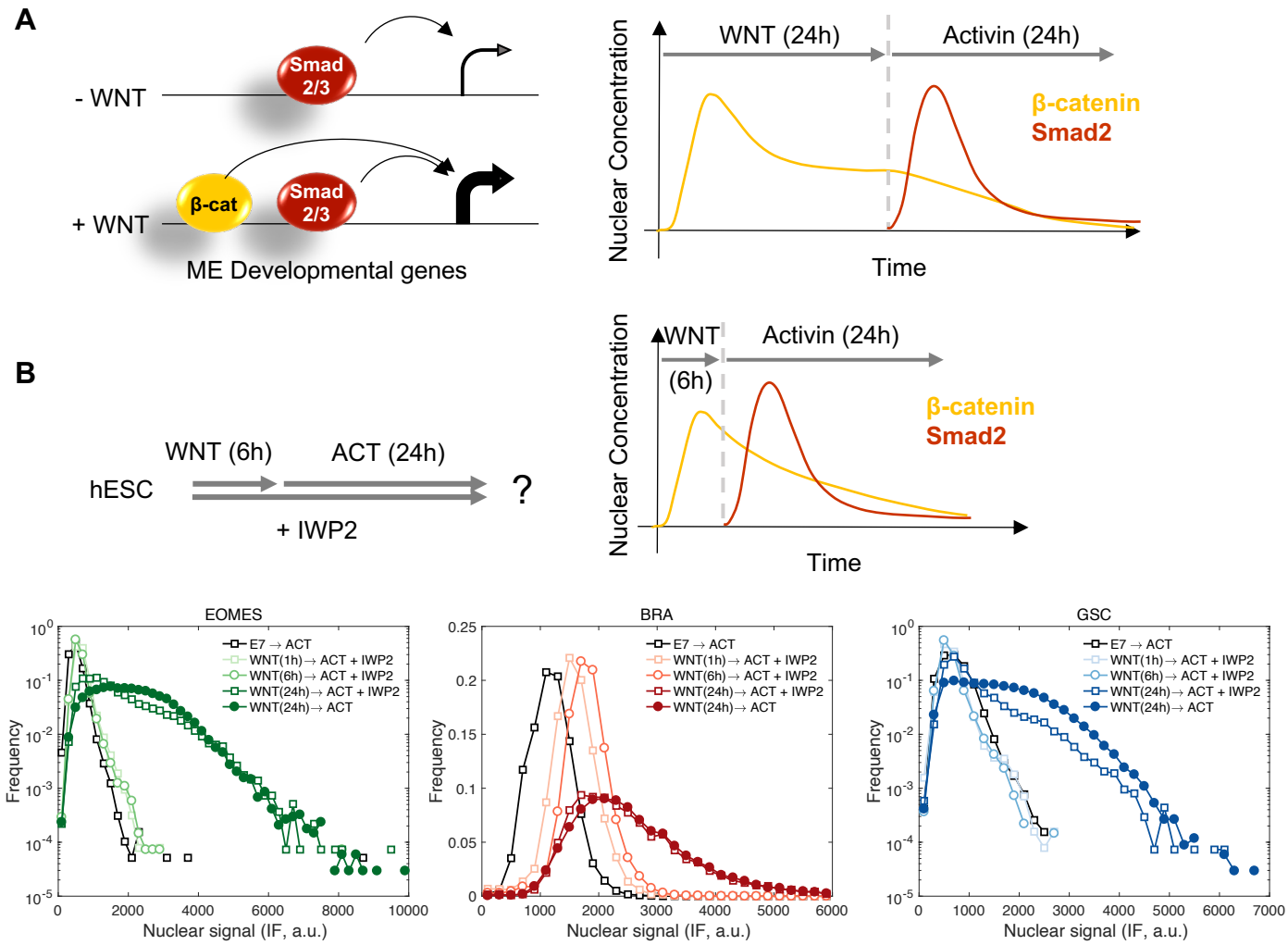
A
- WNT
Smad 2/3
+ WNT
β-cat
Smad 2/3
ME Developmental genes
WNT (24h)
Activin (24h)
Nuclear Concentration
β-catenin
Smad2
Time
B
hESC
WNT (6h)
ACT (24h)
+ IWP2
?
WNT (6h)
Activin (24h)
Nuclear Concentration
β-catenin
Smad2
Time
EOMES
BRA
GSC
E7 → ACT
WNT(1h)→ ACT + IWP2
WNT(6h)→ ACT + IWP2
WNT(24h)→ ACT + IWP2
WNT(24h)→ ACT
Frequency
Nuclear signal (IF, a.u.)

Figure 4

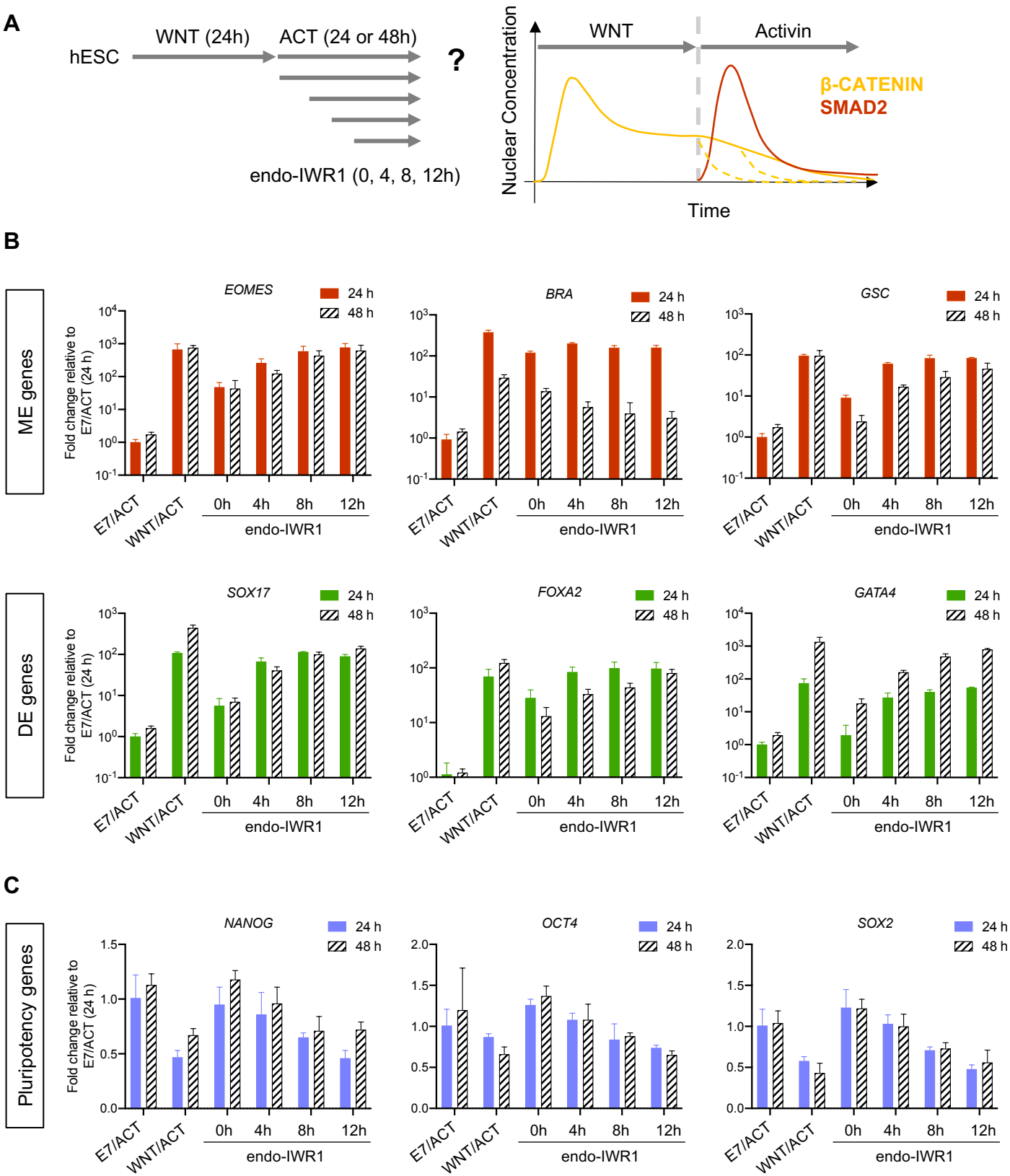
A
hESC
WNT (24h)
ACT (24 or 48h)
?
endo-IWR1 (0, 4, 8, 12h)
WNT
Activin
Nuclear Concentration
β-CATENIN
SMAD2
Time
B
ME genes
EOMES
BRA
GSC
DE genes
SOX17
FOXA2
GATA4
24 h
48 h
Fold change relative to E7/ACT (24 h)
E7/ACT
WNT/ACT
0h
4h
8h
12h
endo-IWR1
C
Pluripotency genes
NANOG
OCT4
SOX2

Figure 5

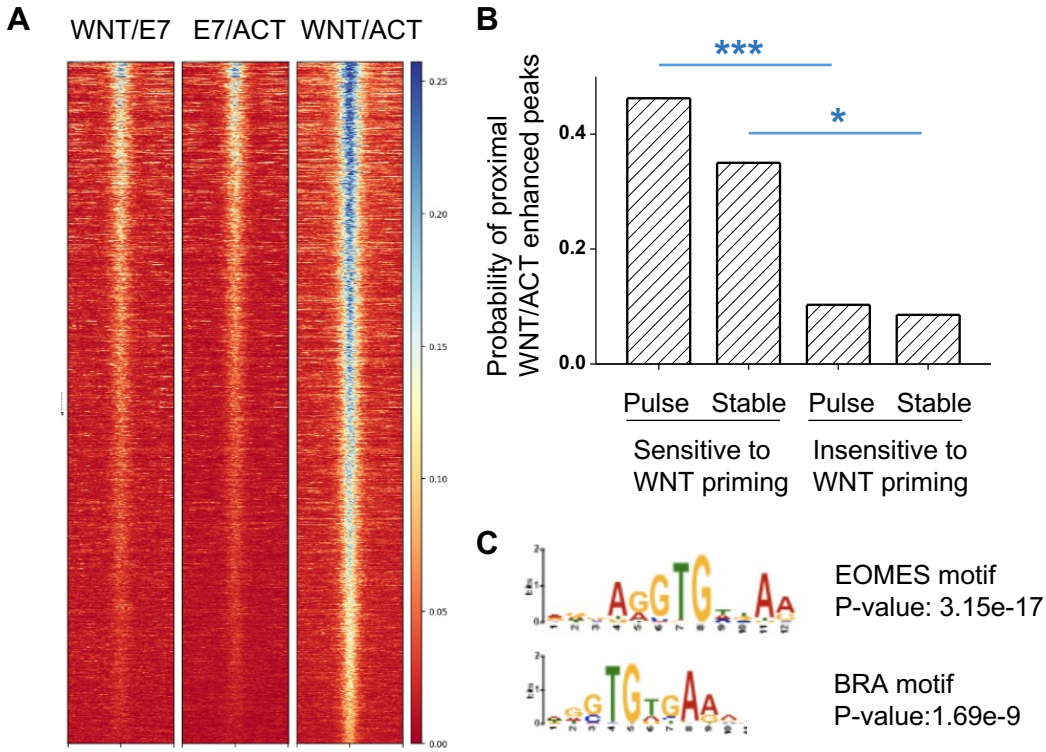
A
WNT/E7
E7/ACT
WNT/ACT
0.25
0.20
0.15
0.10
0.05
0.00
B
***
*
Probability of proximal WNT/ACT enhanced peaks
0.4
0.2
0.0
Pulse
Stable
Pulse
Stable
Sensitive to WNT priming
Insensitive to WNT priming
C
EOMES motif
P-value: 3.15e-17
BRA motif
P-value:1.69e-9

Figure 6

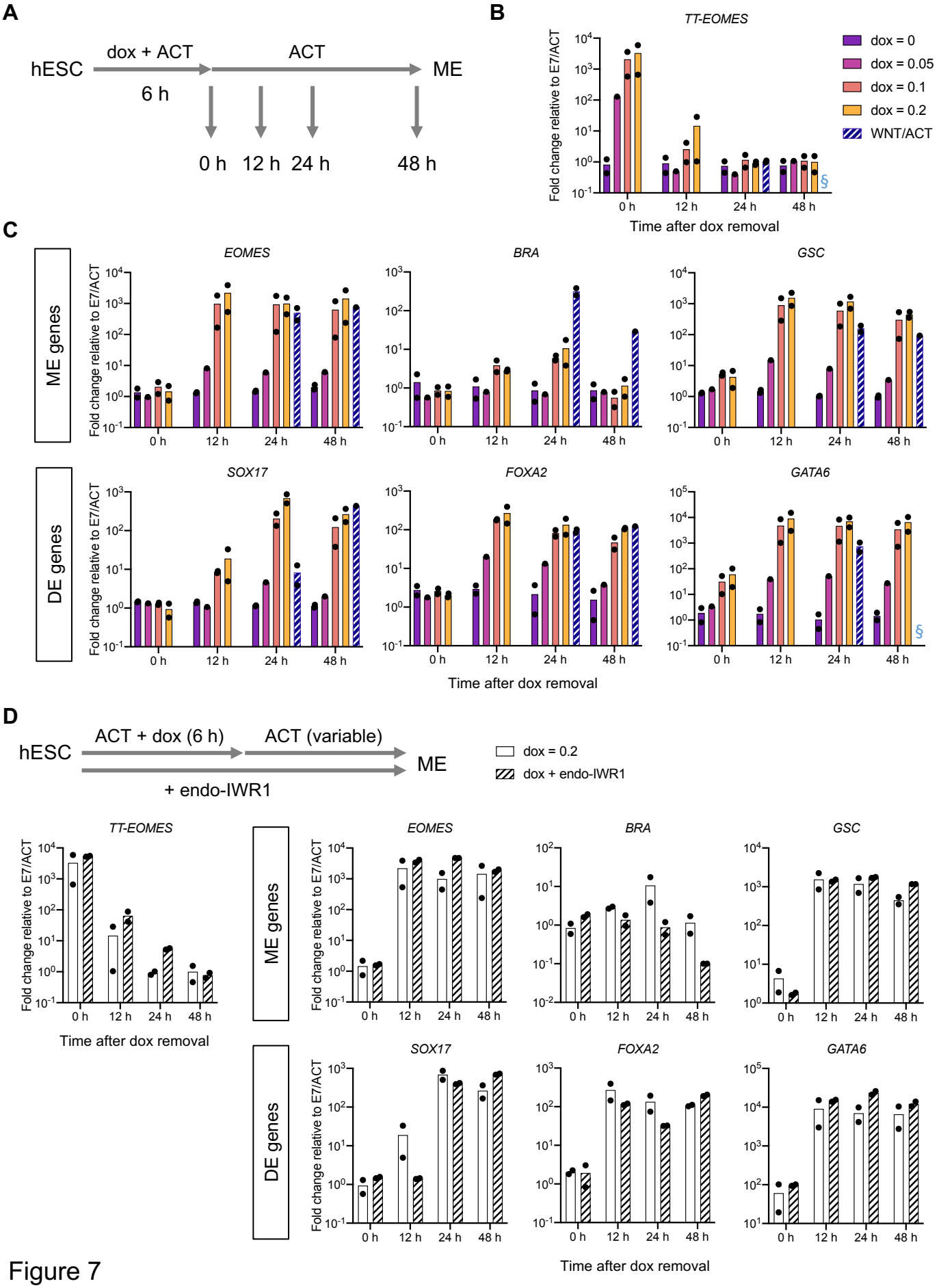
A
hESC
dox + ACT
6 h
ACT
ME
0 h
12 h
24 h
48 h
B
TT-EOMES
Fold change relative to E7/ACT
dox = 0
dox = 0.05
dox = 0.1
dox = 0.2
WNT/ACT
§
Time after dox removal
C
ME genes
DE genes
EOMES
BRA
GSC
SOX17
FOXA2
GATA6
Fold change relative to E7/ACT
Time after dox removal
D
hESC
ACT + dox (6 h)
ACT (variable)
+ endo-IWR1
ME
dox = 0.2
dox + endo-IWR1
TT-EOMES
ME genes
DE genes
EOMES
BRA
GSC
SOX17
FOXA2
GATA6
Fold change relative to E7/ACT
Time after dox removal

Figure 7

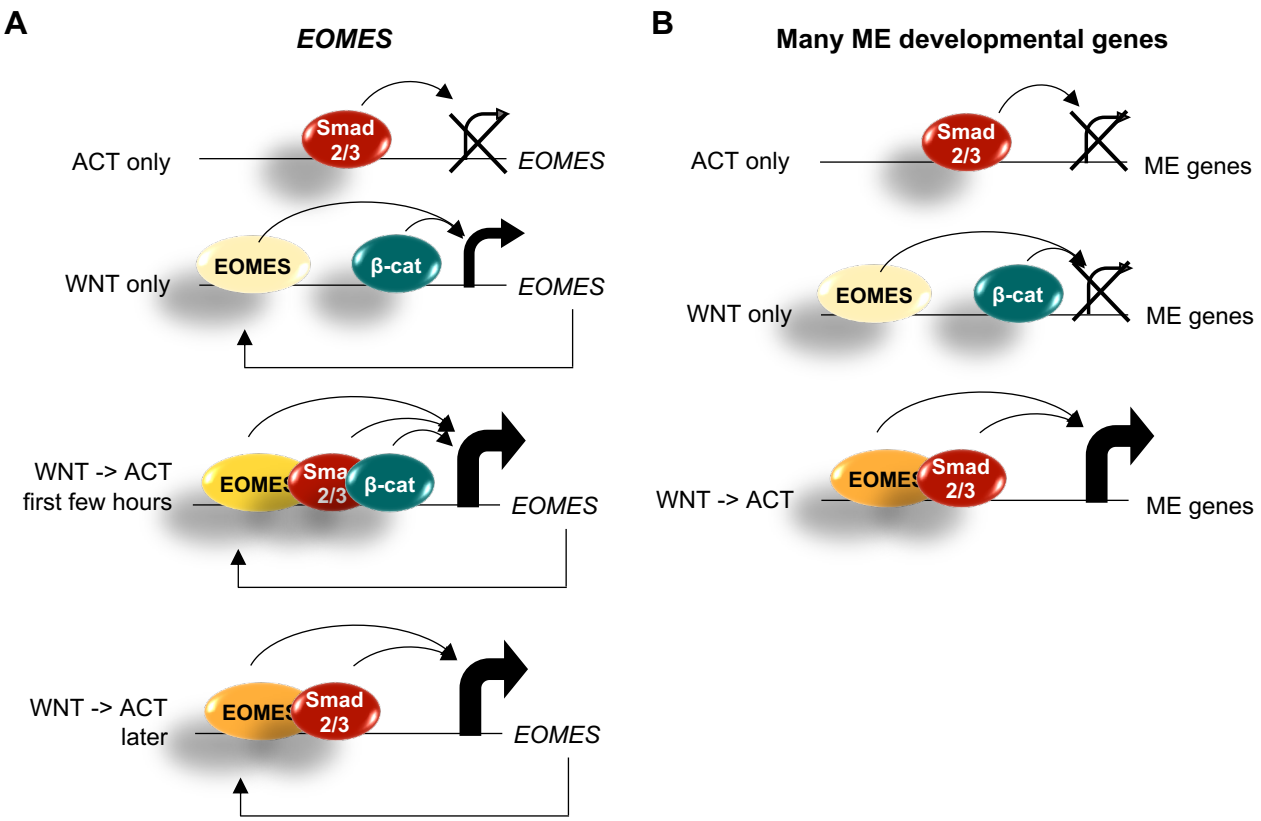
A
EOMES
ACT only
Smad 2/3
EOMES
WNT only
EOMES
β-cat
EOMES
WNT -> ACT first few hours
EOMES
Smad 2/3
β-cat
EOMES
WNT -> ACT later
EOMES
Smad 2/3
EOMES
B
Many ME developmental genes
ACT only
Smad 2/3
ME genes
WNT only
EOMES
β-cat
ME genes
WNT -> ACT
EOMES
Smad 2/3
ME genes

Figure 8